Eur Radiol (2015) 25:736–744
DOI 10.1007/s00330-014-3456-7

EXPERIMENTAL

Quantification of plaque lipids in the aortic root of ApoE-deficient mice by 3D DIXON magnetic resonance imaging in an ex vivo model

Barbara Dietel · Lubos Budinsky · Constanze Kuehn · Michael Uder · Stephan Achenbach · Andreas Hess

Received: 25 May 2014 / Revised: 3 September 2014 / Accepted: 26 September 2014 / Published online: 31 October 2014

Abstract
Objectives To establish a dedicated protocol for the three-dimensional (3D) quantification of plaque lipids in apolipoprotein E-deficient (apoE$^{-/-}$) mice using ex vivo MRI.
Methods ApoE$^{-/-}$ mice were fed a high-fat diet (n=10) or normal food (n=10) for 3 months. Subsequently, a 3D FLASH MRI sequence was used to view the anatomy of the aortic root in the isolated hearts, where a 3D double-echo two-excitation pulse sequence (DIXON sequence) was used to selectively image plaque lipids. The vessel wall, lumen and plaque lipid volumes were quantified by MRI and histology for correlation analysis.
Results DIXON MRI allowed visualisation and accurate quantification of plaque lipids. When comparing the vessel wall, lumen and plaque lipid sizes in the aortic root, Bland–Altman and linear regression analysis revealed a close correlation between MRI results and the histological data both on a slice-by-slice basis and of the volumetric measurements (vessel wall: r^2=0.775, p<0.001; vessel lumen: r^2=0.875; p=0.002; plaque lipid: r^2=0.819, p=0.003).
Conclusions The combination of 3D FLASH and DIXON-sequence MRI permits an accurate ex vivo assessment of the investigated plaque parameters in the aortic root of mice, particularly the lipid content.
Key Points
- *Ex vivo MRI allows high resolution quantification of plaque parameters in mice*
- *DIXON MRI enables visualisation of plaque lipids in the aortic root of mice*
- *A close correlation between histology and MRI quantifies plaque parameters*
- *Preservation of tissue integrity allows additional analysis to be performed*
- *Short measurement time may permit the translation into in vivo measurements*

Keywords Magnetic resonance imaging · Atherosclerotic plaques · Mouse · Animal model · Disease progression

Abbreviations

3D	Three-dimensional
apoE	Apolipoprotein E
CCD	Charge-coupled device
FLASH	Fast low-angle shot
FOV	Field of view
HS	Histology
MRI	Magnetic resonance imaging
NC	Normal chow
RARE	Rapid acquisition with refocused echoes
ROI	Region of interest
TE	Echo time
TR	Repetition time
WD	Western-type diet

B. Dietel (✉) · C. Kuehn · S. Achenbach
Department of Cardiology and Angiology, University Hospital of Erlangen-Nuremberg, Erlangen, Germany
e-mail: Barbara.Dietel@uk-erlangen.de

L. Budinsky
Campus Science Support Facilities (CSF), Vienna Biocenter (VBC), 1030 Vienna, Austria

M. Uder
Department of Radiology, University Hospital of Erlangen-Nuremberg, Erlangen, Germany

A. Hess
Department of Experimental and Clinical Pharmacology and Toxicology, University of Erlangen-Nuremberg, Erlangen, Germany

Introduction

Atherosclerosis progression has been commonly investigated in experimental mouse models such as apolipoprotein E-deficient (apoE$^{-/-}$) mice. These animals rapidly develop atherosclerotic lesions consequent to the knockout of apoE, which is involved in the return transport of cholesterol to the liver [1, 2]. The extent of plaque deposits in the aortic root is a reliable indicator for the overall severity of atherosclerosis. In animal models, magnetic resonance imaging (MRI) has thus far been used mainly to determine the aortic root plaque size both ex vivo [3, 4] and in vivo [5–8]. However, the plaque volume is not the major determining factor of the risk for potential rupture. The atherosclerotic plaque composition might be a more relevant marker of vulnerability [9]. The lipid content has been shown to be among the most relevant parameters for assessing the risk of plaque rupture in patients who suffer from coronary artery disease (CAD) [10]. In several previous studies, MRI was used to quantify the lipid contents of atherosclerotic lesions in larger animals (porcine and rabbit models) [11–13]. In mice, however, atherosclerotic plaque composition analysis remains challenging because of the small size of the mouse aorta. The aortic root diameter, which is approximately 1 mm, requires a considerably higher spatial resolution relative to those of larger animals or humans. To date, very few studies have investigated atherosclerotic plaque components in the established mouse models of atherosclerosis [3, 4, 14]. These studies were either limited by spatial resolution, particular in the third dimension [14], or by a long duration of data acquisition [3, 4]. Consequently, the exact quantification of plaque components, particularly the plaque lipid content, using in vivo measurements remains challenging. Until recently, Oil Red O staining was the gold standard method routinely used to quantify lipid accumulation in the vessel wall [15]. However, the histological approach is tissue-destructive because cross-sections have to be prepared from the aortic root, thus prohibiting further time-resolved analyses of the vascular tissue. In addition, the histological technique is susceptible to tissue artefacts and only allows a two-dimensional analysis of the lipid content, which may inaccurately reflect the true lipid volume. Therefore, the aim of our study was to establish a protocol for the precise three-dimensional (3D) measurement of plaque parameters, especially the lipid content, in the aortic root of mice using ex vivo MRI measurements. Such an approach would preserve tissue integrity and would be potentially suited for in vivo measurements of the atherosclerosis extent and progression both in mice and in humans.

Methods

Animals

All experiments were performed in accordance with European Communities Council Directive (86/609/EEC), and were approved by the local Animal Use and Care Committee (Government of Middle Frankonia, Germany).

Beginning at 6 weeks of age, male apoE$^{-/-}$ mice (Charles River, Sulzfeld, Germany) were fed either normal chow (NC, n=10; control group) or a high-fat Western-type diet (WD, 21 % fat, 1.25 % cholesterol; n=10; atherosclerosis group) for 3 months. The animals were kept on a 12-h light/12-h dark cycle and had free access to food and water. After 3 months, the mice were anaesthetised with isoflurane and transcardially perfused with phosphate buffered saline. For MRI analysis, the hearts were resected and fixed in 1.5-ml caps that had been filled with Roswell Park Memorial Institute (RPMI) 1640 medium to avoid tissue desiccation.

Ex vivo MRI

The isolated hearts were imaged using a 7 T/30 cm horizontal-bore magnet interfaced to a clinical console (ClinScan, Bruker BioSpin; gradient strength, 290 mT/m) running Syngo (Siemens) for the control of MRI workflow and image reconstruction. A circular polarized receive-only quadrature coil optimised for the mouse brain (useful for imaging of objects up to 2 cm in diameter) was used in combination with a circular polarised birdcage body coil for excitation.

First, a localizer sequence was obtained in three orthogonal planes, followed by a 3D spin-echo rapid acquisition with refocusing echoes (RARE) sequence [16] (repetition time (TR), 2 s; echo time (TE), 11 ms; average, 1; turbo factor, 65; measurement time, 12 min) with a 24×24×8 mm field of view (FOV) and a 256×256×80 imaging matrix, which was necessary for aortic root identification. The resulting spatial resolution was near isotropic at 94×94×100 μm. An inversion pulse with inversion time 500 ms was used to enhance the resulting image contrast for better anatomical description of the aortic root. Furthermore, a 3D fast low-angle shot (FLASH) sequence with a double-echo two-excitation pulse sequence for phase-sensitive encoding of fat and water signals (DIXON) [17] (TR, 12 ms; TE_1, 2 ms; TE_2, 3.5 ms; averages, 16; measurement time, 52 min) was acquired in the same FOV and resolution as a RARE sequence. This sequence is characterised by its selective high fat contrast and for this reason serves as a standard sequence in clinical practice [18]. MRI measurements were obtained at a stable temperature (23±2 °C) to prevent further plaque lipid crystallisation. The data acquisition time for the entire MRI protocol was 64 min.

MRI data analysis

On the basis of the obtained data sets, the vessel wall and vessel lumen plaque lipid deposit volumes in the aortic root were determined. A semi-automated workflow was established for data analysis. To replicate a standard histological evaluation, a region of interest (ROI) with a uniform height of 600 μm was defined in the anatomical 3D MRI data sets that encompassed the aortic root. For localisation, typical anatomical landmarks such as the cusps of the aortic valve and the coronary arteries were identified in the MR images. The total vessel wall volume was analysed by segmenting the aortic root on turbo spin images, which enabled the morphological depiction of the vascular wall. For segmentation, the outer and inner boundaries of the vessel wall, which were silhouetted against the surrounding tissue by its reduced T2-weighted signal intensity, were traced manually using data sets obtained from the RARE sequence (Fig. 1A). On the basis of this segmentation, the vessel wall volume between the two boundary lines and the vessel lumen volume were calculated (Fig. 1A). Moreover, this vessel wall segmentation was transferred to the DIXON measurements and served as a volume of interest (VOI) for determining the plaque lipid compartments, which were marked in red (Fig. 3). Consequently, the lipid compartments outside of the aortic root were excluded from evaluation by manual inspection. Lipid compartment segmentation within the VOI was conducted using a marching-cube algorithm with a defined threshold value (30 % of grey-value intensity). This threshold, which was applied on the fat-only images within the VOI, has been proven suitable and reliable for lipid segmentation when using the fat-only images from high-contrast DIXON measurements.

Oil Red O staining of the aortic root

After the MRI measurements were obtained, myocardial tissues were frozen at −80 °C until further use. Cryosections (thickness, 7 μm) were cut from the aortic roots, starting from the branching point of the coronary arteries for a total distance of 600 μm with 50-μm intervals between each section (13 sections per aortic root). After staining with the liposoluble dye Oil Red O for 30 min, sections were rinsed in phosphate buffered saline and mounted with coverslips. Photographic images of Oil Red O-stained histologic sections were obtained using a microscope (Olympus) with a mounted CCD camera (Nikon; resolution, 1,280×960 pixel, RGB image) at a magnification of ×60. The areas of the vessel wall, vessel lumen and plaque lipids were determined manually from the 13 cross-sections using planimetric software (NIS elements, Nikon) to calculate the mean areas. The volumes of the three parameters were estimated by multiplying the mean areas by the applied total evaluation distance (600 μm) and were subsequently compared with the corresponding MRI-determined volumes.

Correlation between MRI and histology

The correlation between the MRI and histological measurements was analysed in a Bland–Altman and linear regression analysis. A slice-by-slice comparison was used to detect agreement between the matched histological and MRI sections. For this purpose, both methods (MRI and histology) were used to quantify the areas of the vessel wall and plaque lipids from 12 independent slices. In addition, correlations between the histology and MRI-based 3D vessel wall, vessel lumen and plaque lipid quantifications were also assessed in a Bland–Altman and linear regression analysis.

Statistics

The statistical analysis was performed with SPSS software (IBM, Berlin, Germany). Kolmogorov–Smirnov test served as normality test. The statistical significance of differences between the NC and WD groups were detected using Student's *t* test. A linear regression and Bland–Altman analysis were used to evaluate correlations. Data were expressed as mean±standard errors of measurement (SEM). A *P* value of less than 0.05 was considered statistically significant.

Results

Correlation of histological slices with the corresponding MR images

In order to validate whether the MRI sequences with the described parameters were suitable for vessel wall, vessel lumen and plaque lipid deposit volume quantification, we first qualitatively compared images from histological cross-sections with the corresponding MR images. As shown in Fig. 1A.a, the aortic root structure was well visualised with the applied RARE sequence. Accordingly, on the MR images, the vessel wall was distinguishable from the surrounding tissue and vessel lumen by the enhanced contrast. The identification of the inner and outer wall boundaries enabled segmentation of the vessel wall (Fig. 1A.b). Regarding morphology, the MR images (Fig. 1A.a) matched the corresponding histological sections (Fig. 1A.d).

On DIXON measurement data sets, plaque lipids were visible as white areas (Fig. 1 A.c). A comparison of images from DIXON data sets and the matched histological sections (Fig. 1A.d) demonstrated that the lipid-rich areas detected by MRI corresponded to the red-coloured regions in the Oil Red O-stained sections.

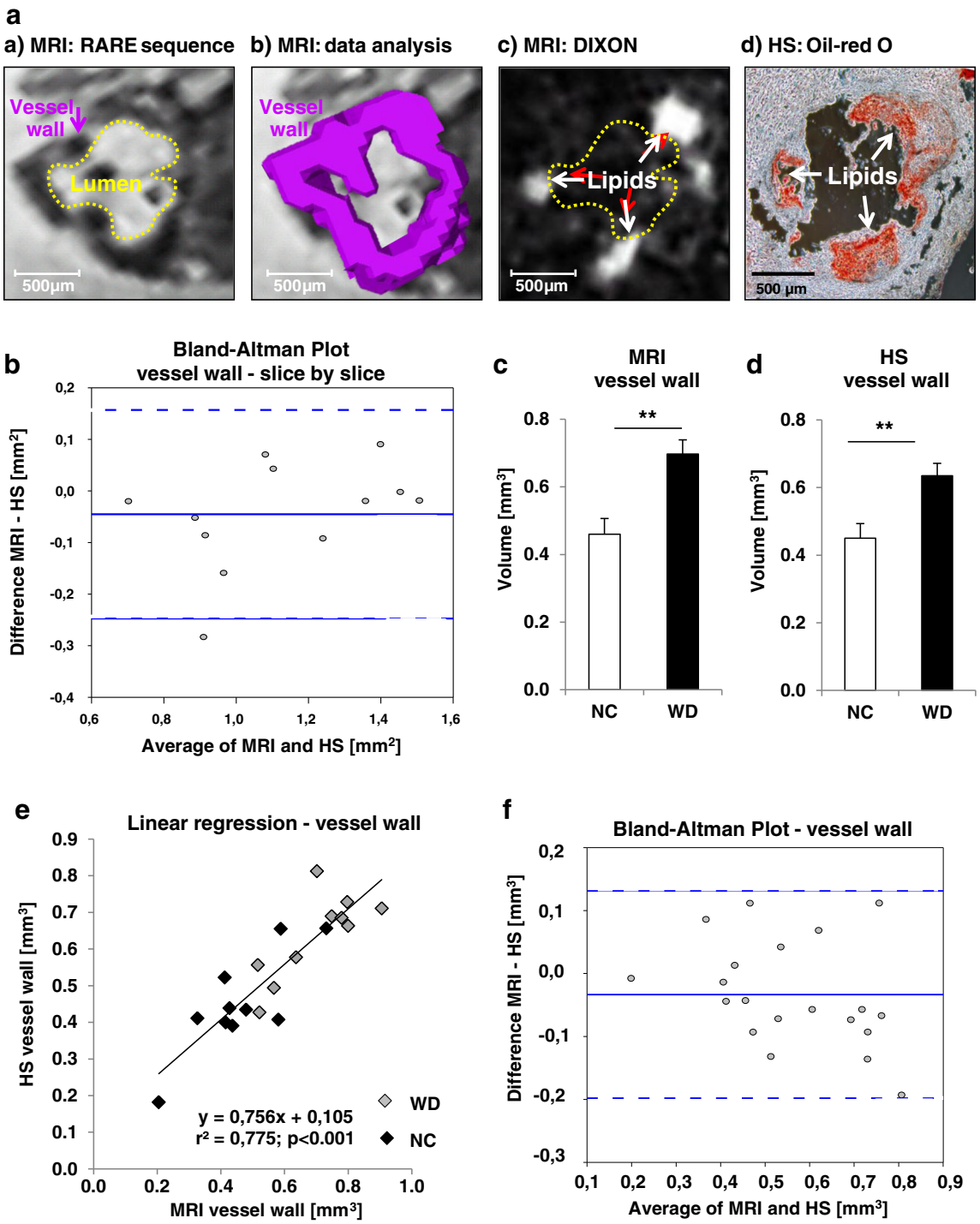

Fig. 1 Illustration of the aortic root and its plaque lipid content via ex vivo MRI of the isolated heart. **A** Comparison of histological sections with the corresponding MRI sections. *a* MR RARE sequence illustrating the anatomy of the aortic root, the *black area* corresponds to the vessel wall, which contains incorporated lipid-rich plaques. The *yellow dotted line* marks the borderline between the vessel wall and the lumen. *b* Vessel wall segmentation using data sets obtained from the MR RARE sequence. *c* DIXON measurements of the aortic root generate a white signal in lipid-rich areas of the vessel wall (*white arrows*) in the fat-only picture, which is used to quantify plaque lipid volume. *d* Oil Red O staining of the aortic root shows red-coloured lipid accumulation in the vessel wall (*white arrows*) and is consistent with the DIXON measurements. **B** Bland–Altman assessment of the difference between the MRI- and histology-based slice-by-slice quantifications of the vessel wall area, showing mean (*solid line*)±STABW (*dotted line*). **C** MRI data quantification shows a 1.5-fold increase in the vessel wall volume in WD relative to NC mice, whereas histology (HS) shows a 1.4-fold increase **D**. Bland–Altman (**E**) and linear regression analysis (**F**) of the difference between MRI and histology-based volumetric vessel wall measurements. *NC* normal chow, *WD* Western-type diet, *HS* histology; $^{**}p<0.01$; $n=10$ NC vs. 10 WD mice

Three-dimensional vessel wall analysis

Data sets obtained from the RARE sequence were evaluated to quantify the vessel wall volume. The Bland–Altman analysis, which was used to assess correlations between histological and MRI sections on a slice-by-slice basis, showed a close agreement between the histological and MRI-based vessel wall area detection methods (Fig. 1B). The linear regression analysis confirmed the correlation between the two methods (r^2=0.897; data not shown), indicating that the applied parameters were suitable for 3D vessel wall quantification by ex vivo MRI.

3D vessel wall segmentation at a defined evaluation height of 600 μm (300 μm around the common carotid artery) showed a significant 1.5-fold increase in the total vessel wall volume from 0.46±0.04 mm^3 in the NC mice to 0.69±0.04 mm^3 in the WD mice (Fig. 1C, p<0.01).

In comparison, the histological assessment was based on the evaluated mean vessel wall area, which was used to determine 3D vessel wall size. We detected a significant 1.4-fold increase in the vessel wall volume from 0.45±0.04 mm^3 in NC mice to 0.64±0.03 mm^3 in WD mice (Fig. 1D). The linear regression analysis revealed a significant correlation between MRI-based and histologically measured vessel wall volumes (Fig. 1E; r^2=0.775, p<0.001). The observed close agreement between the two methods was confirmed in a Bland–Altman analysis (Fig. 1F). A visual inspection of the histological sections revealed no necrotic regions within the atherosclerotic lesions.

Quantification of the vessel lumen in the aortic root

The vessel lumen volume was also assessed using both histology and the RARE-sequence MRI data sets. The MRI measurements revealed a volume of 0.52±0.05 mm^3 in NC mice compared to 0.43±0.04 mm^3 in WD mice (Fig. 2 A; p=0.197). Accordingly, the vessel lumens in WD mice had a vessel lumen size 83 % of that in NC mice.

The histological assessment revealed that WD mice had a vessel lumen size 78 % of that in NC mice. While the vessel

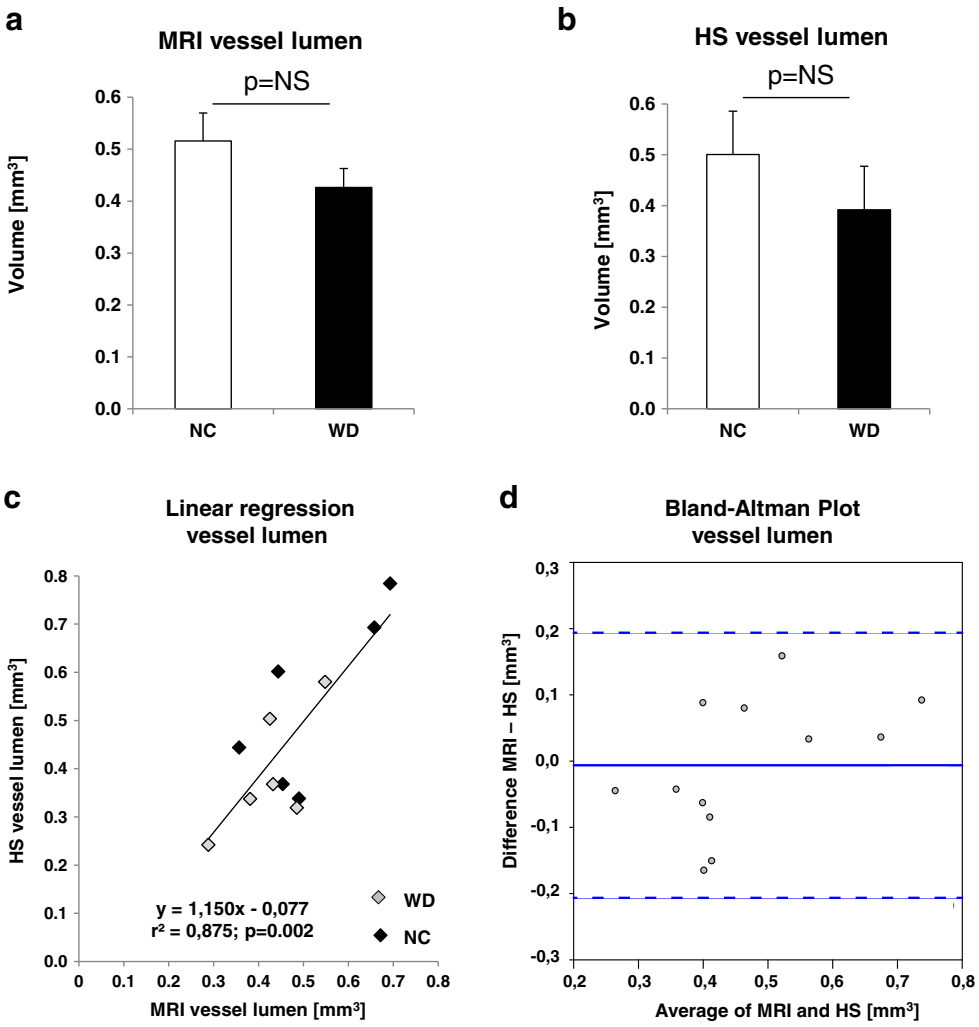

Fig. 2 Comparison of the MRI-based and histological vessel lumen quantification. MRI shows a 17 % decrease in the vessel lumen of WD mice relative to that of NC mice (**A**), whereas the histological evaluation (HS) reveals a 22 % reduction (**B**). Bland–Altman (**C**) and linear regression analysis (**D**) of the difference between the MRI- and histology-based volumetric vessel lumen measurements. *NS* not significant, *NC* normal chow, *WD* Western-type diet, *HS* histology, n=6 NC vs. 6 WD mice

lumen volume was 0.50±0.08 mm^3 in NC mice, the WD mice had a mean vessel lumen volume of 0.39±0.05 mm^3 (Fig. 2B; p=0.265). A linear regression analysis (Fig. 2C) revealed that the MRI-quantified vessel lumen volume correlated significantly with the histologically quantified volume (r^2=0.875, p=0.002). As shown in Fig. 2D, the Bland–Altman analysis revealed that the magnitudes of the differences between the two methods remained constant throughout the range of measurement.

Lipid content quantification in the aortic root by MRI

The lipid volumes were measured by segmenting the lipid compartments within the aortic wall boundaries as depicted by the DIXON measurements. Figure 3 shows the lipid contents both in an aortic root cross-section (Fig. 3A) and a 3D view (Fig. 3B). Compared to the NC mice (Fig. 3, left), the WD mice exhibited a significant increase in the plaque lipid volume in the aortic root vessel wall (Fig. 3, right).

A slice-by-slice comparison of both methods in a Bland–Altman analysis revealed a close correlation between the calculated plaque lipid areas (Fig. 4A).

The MRI-based quantification yielded a mean lipid volume of 0.035±0.014 mm^3 in NC mice compared with 0.124±0.029 mm^3 in WD mice (Fig. 4B, p<0.01), which corresponds to a 3.5-fold increase in plaque lipid volume in response to a high-fat diet. The plaque lipid volumes calculated according to the histological measurements were 0.041±0.012 mm^3 in NC mice and 0.131±0.024 mm^3 in WD mice (Fig. 4C, p<0.01), corresponding to a 3.2-fold increase in the lipid volume in the latter group. A linear regression analysis demonstrated a significant relationship between the histologically determined and DIXON MRI-quantified lipid volumes (Fig. 4D; r^2=0.819, p=0.003). A close correlation was also demonstrated in a Bland–Altman analysis (Fig. 4E).

Discussion

The lipid content of atherosclerotic lesions is an important predictor of the potential risk for plaque rupture. Given the small size of the mouse aorta, the quantification of plaque lipids in the established apoE$^{-/-}$ mouse model has previously been difficult. In the present study, we investigated the feasibility of ex vivo DIXON measurements, in which phase-sensitive encoding resulted in specific fat and water contrast images of the isolated heart that could be used to quantify the aortic root lipid content in apoE$^{-/-}$ mice. Because of the selective fat contrast and the short scan times, the approach validated herein may even be suitable for future in vivo measurements. To further reduce the measurement time, we performed digital resampling and found that even a quarter of the applied MRI resolution was sufficient to determine lipid plaque content. Therefore, the ex vivo measurement time could be reduced from 64 to 16 min, thus enabling an

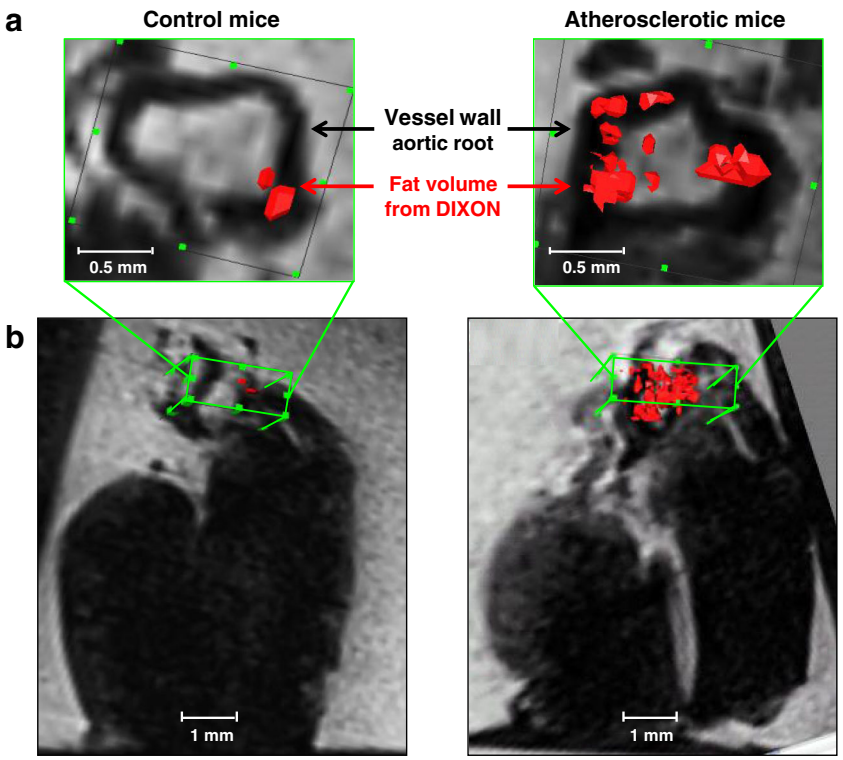

Fig. 3 Plaque lipid segmentation using the DIXON sequence. **A** MR RARE images of exemplary aortic root cross-sections with red-coloured plaque lipids that were obtained from the DIXON data sets of an NC (*left*) and a WD mouse (*right*). **B** MR RARE images of exemplary cardiac coronal sections from an NC (*left*) and a WD mouse (*right*). 3D illustration of DIXON-measured lipid compartments (*red*) in the region of interest (*green*), which includes the aortic root. *NC* normal chow, *WD* Western-type diet

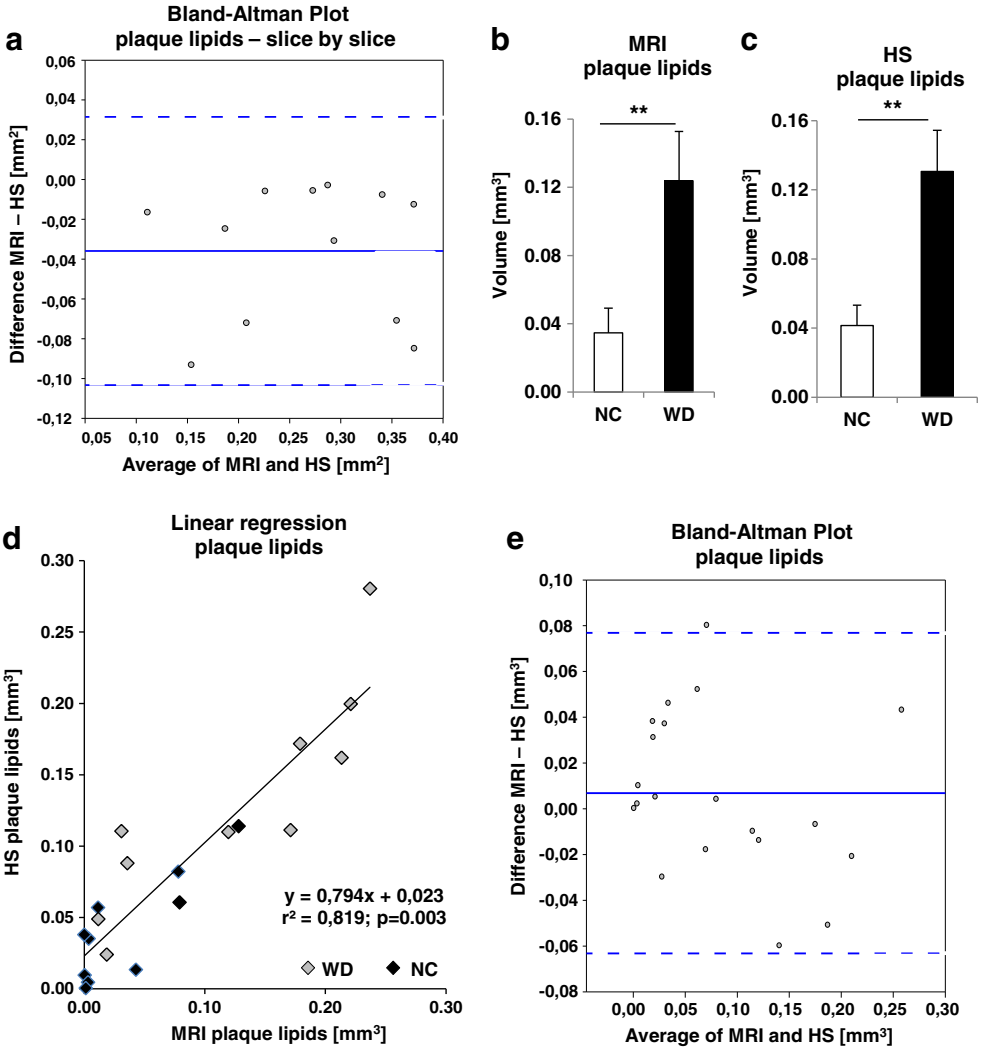

Fig. 4 Comparison of MRI-based and histological lipid quantification results. MRI shows a 3.5-fold increase in plaque lipids in WD compared to NC mice (**A**), whereas histology (HS) shows a 3.2-fold increase (**B**). Bland–Altman (**C**) and linear regression analysis (**D**) of the difference between the MRI and histology-based volumetric plaque lipid measurements. *NC* normal chow, *WD* Western-type diet, *HS* histology; $^{**}p<0.01$; $n=10$ NC vs. 10 WD mice

in vivo measurement duration of approximately 30 min, including ECG-gating.

For several years, non-invasive MRI has been used to investigate the progression of atherosclerotic lesions both in humans suffering from CAD and in animal models. Fayad et al. reported the use of MRI to assess atherosclerotic lesions in genetically engineered mice as early as 1998 [19]. The authors observed close agreement between MRI and histology-based measurements of the vessel wall area in the abdominal aorta and the iliac artery. Further studies conducted in mice, rabbits and porcine models confirmed the feasibility of MRI for analysing essential plaque parameters such as the vessel wall thickness, total vessel area and luminal area [6, 11, 12, 20, 21]. However, only few studies have addressed the quantification of plaque lipids in the established mouse models of atherosclerosis, which is amongst the most important parameters to assess the risk of plaque rupture [22–24]. The previous studies used spatial resolutions that hindered appropriate 3D quantification or scan times that were much too long for in vivo measurements. One of the major challenges to the establishment of suitable MR sequences for plaque lipid quantification is the small arterial size in mice, which introduces the requirement for high contrast in order to obtain reliable results within relatively short scan times. In our study, we have shown that a combination of a RARE sequence for aortic root localisation and DIXON measurements for selective lipid illustration was suitable for the quantification of incorporated lipids. A comparison of the MRI-measured vessel wall, lumen and plaque lipid volumes found close correlations with the results obtained from the gold-standard histology. In contrast to a former study by McAteer et al., who also described an ex vivo MRI-based approach for plaque lipid quantification, the total measurement time in our study was considerably shorter (64 min versus 7 h) [3]. In the study by McAteer et al., the lipid-rich regions of the aortic root and the descending aorta were identified using a multi-echo sequence according to the low-signal areas on grey-scale MR images. However, the prolonged imaging time precluded the translation of this approach into in vivo MRI. Investigating various contrast mechanisms, Schneider et al. found that T1-

weighted measurements were superior to T2-weighted contrast imaging for quantifying both lipid-rich and fibrous areas of the plaque [4], which was in accordance with former studies of human atherosclerotic plaques [25–27]. However, given the total measurement time of 10 h, in vivo application of this method is also not possible. Trogan et al. investigated plaque size and composition using in vivo multi-contrast MRI in a mouse model from a combination of T1, T2 and proton density (PD)-weighted images. Lipid-rich areas in the thoracic aorta were identified by hyperintense signals on T1-weighted images and hypointense signals on T2- and PD-weighted images [14]. Motion artefacts, which compromise in vivo MRI measurements, were suppressed by cardiac and respiratory gating. The applied parameters allowed lipid and collagen content quantification in living mice, thus demonstrating enormous progress with respect to the characterisation of plaque composition. However, the large slice thickness of 500 μm limited the precision of this method with regard to 3D quantification. Therefore, an overestimation of the fibrous content was reported. This possible source of error was greatly reduced in our study with the use of a slice thickness of 100 μm, which permitted a nearly isotropic voxel size and thus a more precise volumetric assessment. Accordingly, the slice-by-slice analysis that we performed revealed a close correlation between the results from histology and MRI, thus confirming that the histological and MRI sections were closely matched. Furthermore, the DIXON technique, which we applied for plaque lipid quantification, is a dedicated fat content measurement protocol, which enables the discrimination of fat and water in a proton resonance frequency-based manner through the summation and subtraction of in-phase and out-of-phase images [18]. However, a major challenge during the last two decades was the sensitivity of the DIXON technique to magnetic field heterogeneity, inhibiting a complete separation of fat and water. Accordingly, the accumulation of an additional phase between the two echoes, which resulted from field heterogeneities, caused a contamination of the fat images by water images and vice versa. To identify and remove this phase, region growing-based post-processing algorithms yielded considerable improvement, overcoming the weakness of this technique by removing the effects of field heterogeneity [28].

Given these advantages, DIXON acquisition is now routinely applied in clinical settings such as the detection of cardiac fat content and lipomatous infiltration of the myocardium [29]. Some of the important advantages of the DIXON technique over conventional previous approaches, such as multi-echo, T2, and PD-weighted imaging, with respect to aortic root lipid quantification include an enhanced microscopic fat contrast and a reduced artefact incidence at a high 3D resolution. In our study, a strong correlation between the histology and MRI-based 3D plaque lipid quantification demonstrated the accuracy of the applied DIXON measurements.

In conclusion, our study results demonstrate the suitability of the DIXON sequence for precise lipid volume quantification in the aortic root of apoE$^{-/-}$ mice via ex vivo MRI. The short measurement time is an initial step towards the future translation of this technique into in vivo applications in order to analyse the extent and progression of atherosclerotic lesions in both murine experimental atherosclerosis models and in humans.

Acknowledgments The authors would like to thank Regina Altendorf for her exceptional technical assistance. The project was funded by the German Foundation of Heart Research (F/25/13) and the ELAN-fonds (M2-12-12-19-1) of the University of Erlangen-Nuremberg.

The scientific guarantor of this publication is Dr. Barbara Dietel. The authors of this manuscript declare no relationships with any companies whose products or services may be related to the subject matter of the article. No complex statistical methods were necessary for this paper. Institutional review board approval was not required because it did not contain analysis of human tissue. Approval from the institutional animal care committee was obtained. Methodology: prospective, experimental, performed at one institution.

References

1. Zhang SH, Reddick RL, Piedrahita JA, Maeda N (1992) Spontaneous hypercholesterolemia and arterial lesions in mice lacking apolipoprotein E. Science 258:468–471
2. Wouters K, Shiri-Sverdlov R, van Gorp PJ, van Bilsen M, Hofker MH (2005) Understanding hyperlipidemia and atherosclerosis: lessons from genetically modified apoe and ldlr mice. Clin Chem Lab Med 43:470–479
3. McAteer MA, Schneider JE, Clarke K, Neubauer S, Channon KM, Choudhury RP (2004) Quantification and 3D reconstruction of atherosclerotic plaque components in apolipoprotein E knockout mice using ex vivo high-resolution MRI. Arterioscler Thromb Vasc Biol 24:2384–2390
4. Schneider JE, McAteer MA, Tyler DJ et al (2004) High-resolution, multicontrast three-dimensional-MRI characterizes atherosclerotic plaque composition in ApoE-/- mice ex vivo. J Magn Reson Imaging 20:981–989
5. Alsaid H, Sabbah M, Bendahmane Z et al (2007) High-resolution contrast-enhanced MRI of atherosclerosis with digital cardiac and respiratory gating in mice. Magn Reson Med 58:1157–1163
6. Chaabane L, Pellet N, Bourdillon MC et al (2004) Contrast enhancement in atherosclerosis development in a mouse model: in vivo results at 2 Tesla. MAGMA 17:188–195
7. Choudhury RP, Fayad ZA, Aguinaldo JG et al (2003) Serial, noninvasive, in vivo magnetic resonance microscopy detects the development of atherosclerosis in apolipoprotein E-deficient mice and its progression by arterial wall remodeling. J Magn Reson Imaging 17:184–189
8. Dietrich T, Hucko T, Bourayou R et al (2009) High resolution magnetic resonance imaging in atherosclerotic mice treated with ezetimibe. Int J Cardiovasc Imaging 25:827–836
9. Fuster V, Stein B, Ambrose JA, Badimon L, Badimon JJ, Chesebro JH (1990) Atherosclerotic plaque rupture and thrombosis. Evolving concepts. Circulation 82:II47–II59
10. Guyton JR, Klemp KF (1996) Development of the lipid-rich core in human atherosclerosis. Arterioscler Thromb Vasc Biol 16:4–11

11. Worthley SG, Helft G, Fuster V et al (2000) Noninvasive in vivo magnetic resonance imaging of experimental coronary artery lesions in a porcine model. Circulation 101:2956–2961
12. Worthley SG, Helft G, Fuster V et al (2000) Serial in vivo MRI documents arterial remodeling in experimental atherosclerosis. Circulation 101:586–589
13. Phinikaridou A, Ruberg FL, Hallock KJ et al (2010) In vivo detection of vulnerable atherosclerotic plaque by MRI in a rabbit model. Circ Cardiovasc Imaging 3:323–332
14. Trogan E, Fayad ZA, Itskovich VV et al (2004) Serial studies of mouse atherosclerosis by in vivo magnetic resonance imaging detect lesion regression after correction of dyslipidemia. Arterioscler Thromb Vasc Biol 24:1714–1719
15. Nunnari JJ, Zand T, Joris I, Majno G (1989) Quantitation of oil red O staining of the aorta in hypercholesterolemic rats. Exp Mol Pathol 51:1–8
16. Hennig J, Nauerth A, Friedburg H (1986) RARE imaging: a fast imaging method for clinical MR. Magn Reson Med 3:823–833
17. Dixon WT (1984) Simple proton spectroscopic imaging. Radiology 153:189–194
18. Szumowski J, Coshow WR, Li F, Quinn SF (1994) Phase unwrapping in the three-point Dixon method for fat suppression MR imaging. Radiology 192:555–561
19. Fayad ZA, Fallon JT, Shinnar M et al (1998) Noninvasive in vivo high-resolution magnetic resonance imaging of atherosclerotic lesions in genetically engineered mice. Circulation 98:1541–1547
20. Itskovich VV, Choudhury RP, Aguinaldo JG et al (2003) Characterization of aortic root atherosclerosis in ApoE knockout mice: high-resolution in vivo and ex vivo MRM with histological correlation. Magn Reson Med 49:381–385
21. Sigovan M, Kaye E, Lancelot E et al (2012) Anti-inflammatory drug evaluation in ApoE-/- mice by ultrasmall superparamagnetic iron oxide-enhanced magnetic resonance imaging. Invest Radiol 47: 546–552
22. Falk E (1992) Why do plaques rupture? Circulation 86:III30–III42
23. Kolodgie FD, Burke AP, Farb A et al (2001) The thin-cap fibroatheroma: a type of vulnerable plaque: the major precursor lesion to acute coronary syndromes. Curr Opin Cardiol 16: 285–292
24. Virmani R, Burke AP, Farb A (1999) Plaque rupture and plaque erosion. Thromb Haemost 82:1–3
25. Serfaty JM, Chaabane L, Tabib A, Chevallier JM, Briguet A, Douek PC (2001) Atherosclerotic plaques: classification and characterization with T2-weighted high-spatial-resolution MR imaging–an in vitro study. Radiology 219:403–410
26. Toussaint JF, Southern JF, Fuster V, Kantor HL (1995) T2-weighted contrast for NMR characterization of human atherosclerosis. Arterioscler Thromb Vasc Biol 15:1533–1542
27. Morrisett J, Vick W, Sharma R et al (2003) Discrimination of components in atherosclerotic plaques from human carotid endarterectomy specimens by magnetic resonance imaging ex vivo. Magn Reson Imaging 21:465–474
28. Jellus V (2009) Phase correction method. US Patent Application US 2009/0201021. http://www.freepatentsonline.com/y2009/0201021.html
29. Farrelly C, Shah S, Davarpanah A, Keeling AN, Carr JC (2012) ECG-gated multiecho Dixon fat-water separation in cardiac MRI: advantages over conventional fat-saturated imaging. AJR Am J Roentgenol 199:W74–W83